Chapter 13

ZnO Nanorods as an Intracellular Sensor for pH Measurements

M. Willander and Safaa Al-Hilli

Summary

High-density ZnO nanorods of 60–80 nm in diameter and 500–700 nm in length grown on the silver-coated tip of a borosilicate glass capillary (0.7 μm in diameter) demonstrate a remarkable linear response to proton H_3O^+ concentrations in solution. These nanorods were used to create a highly sensitive pH sensor for monitoring in vivo biological process within single cells. The ZnO nanorods exhibit a pH-dependent electrochemical potential difference versus an Ag/AgCl microelectrode. The potential difference was linear over a large dynamic range (pH, 4–11) and had a sensitivity equal to 51.88 mV/pH at 22°C, which could be understood in terms of changes in surface charge during protonation and deprotonation. Vertically grown nanoelectrodes of this type can be smoothly and gently applied to penetrate a single living cell without causing cell apoptosis.

Key words: Intracellular pH, ZnO nanorods, Potentiometric measurement, pH of adipocyte or fat cell

1. Introduction

One-dimensional (1D) nanostructure research has elucidated many biomarkers that have the potential to greatly improve disease diagnosis *(1–3)*. pH sensor miniaturization is highly important because the large surface-to-volume ratio leads to a short diffusion distance of the analyte toward the electrode surface, thereby providing an improved signal-to-noise ratio, faster response time, enhanced analytical performance, and increased sensitivity *(4)*. These results enable the sensitive and rapid detection of biochemical and physiological processes, essential to basic biomedical research applications. However, our research is at a very primitive stage and many additional efforts are necessary to obtain reliable instrumentation for intracellular measurements.

James Weifu Lee and Robert S. Foote (eds.), *Micro and Nano Technologies in Bioanalysis*,
Methods in Molecular Biology, vol. 544
DOI 10.1007/978-1-59745-483-4_13,

The sensor in this study was used to detect and monitor real changes in cell behavior using changes in the electrochemical potential at the single cell/ZnO nanorod surface interface in the intracellular microenvironment.

When a solid emerges in a polar solvent or an electrolyte, a surface charge will develop through one or more of the following mechanisms: preferential adsorption of ions; dissociation of surface charged species; isomorphic substitution of ions; accumulation or depletion of electrons at the surface; and physical adsorption of charged species onto the surface. The polar and nonpolar surface structures of ZnO nanorods are of interest in understanding the mechanism of interaction of these surfaces with the medium surrounding them. The sensing mechanism is the polarization-induced bound surface charge by interaction with the polar molecules in the liquids. Significant progress in understanding the surface properties of ZnO was achieved recently *(5–15)* stimulated by the importance of this material for a number of applications ranging from cosmetics and medicine to heterogeneous catalysis. ZnO crystallizes in the hexagonal wurtzite structure with lattice parameters (a = 3.25 Å and c = 5.206 Å). ZnO is a polar crystal whose polar axis is the c-axis, and it belongs to the $C_{6v}^4 = p6_3\,mc$ space group.

A practical application of some metal oxides is associated with their pH sensitivity. These oxides (insoluble and stable in water) may function as metal oxide pH electrodes on electronically conducting substrates (not necessarily on the metal from which they are formed). This group of pH sensors is distinguished from metal/metal oxide pH-sensitive electrodes by a different kind of reaction determining their potential-pH response. In this case, a metal oxide/metal oxide (higher and lower valency) couple instead of a metal/metal oxide couple is involved in the pH-dependent equilibrium *(16)*. The oxide layer that covers the electronic conductor contains a mixture of both oxides, one with some oxygen deficiency.

In zero-current potentiometry, the relative size of the two electrodes is immaterial *(17)*. Acquiring useful information in this case requires only that the potential of the working electrode be measured against a well-defined and stable potential from a reference electrode. The conventional reference electrode consists of an electrode of the second type, such as the Ag/AgCl/KCl system. Any foreign potential inadvertently present within the measuring circuit can contaminate the information, as a result, it is mandatory that the reference electrode be placed as close to the working electrode as practically possible. A determination by direct potentiometric measurement is accomplished either by calibrating the electrode with solutions of known concentration or by using the techniques of standard addition or standard subtraction.

An advantage of ZnO nanorod sensors is their small size, which allows intracellular sensing of physiological and biological

parameters in nanoenvironments, and a strong, stable, and reversible signal with respect to pH changes. The detection sensitivity of the pH sensor is achieved by monitoring minimal changes in electrochemical potential caused by binding of biomolecular species on the surfaces of the probe, owing to the high isoelectric point of the material comprising the sensor (in the case of ZnO, the isoelectric point is between 9 and 10) *(18)*.

1.1. Intracellular pH

The acid and base properties of electrolytes in living cells play an important role in any biological process, because the pH value is the most critical parameter in chemical and biochemical reactions. Intracellular pH has been studied extensively for longer than a century, using a wide range of techniques. These techniques have been subject to constant improvements, to the extent that useful measurements can now be made in the smallest of cells. Although intracellular pH changes were observed much earlier, the first measurements of what could loosely be described as intracellular pH were made around 1910 using cell extracts and platinum/hydrogen electrodes (for a review, *see* **ref.** *(19)*). High electrical resistance, however, presented a major problem for the miniaturization of metal minielectrodes. It was not until the 1950s that significant progress was made in producing microelectrodes that could be widely used. pH-sensitive glass, although discovered around 1900, became the material of choice. It has relatively low electrical resistance; no sensitivity to oxidizing and reducing agents, dissolved gasses, anions, or buffers; and it is stable and can produce a relatively rapid response. The electrode consisted of a portion of exposed pH-sensitive glass, which is approximately 500-μm long (*see* **Fig. 1**). Improvements in both the pH-sensitive glass and input impedance of modern electrometers allowed the exposed length of the pH-sensitive glass to be reduced to approximately 100 μm, but the use of these electrodes was restricted to giant cells. The first true pH-sensitive *micro*electrode was produced in 1974 by Thomas *(20)* (*see* **Fig. 2**). Thomas introduced a design wherein the exposed length of pH-sensitive glass (still at least 100

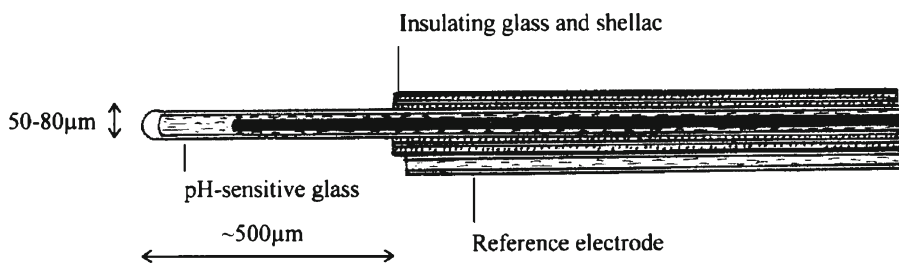

Fig. 1. Glass pH-sensitive electrode used by Caldwell *(19)* to measure intracellular pH in crab muscle fibers. Reproduced from ref. *(19)* with permission from PMC.

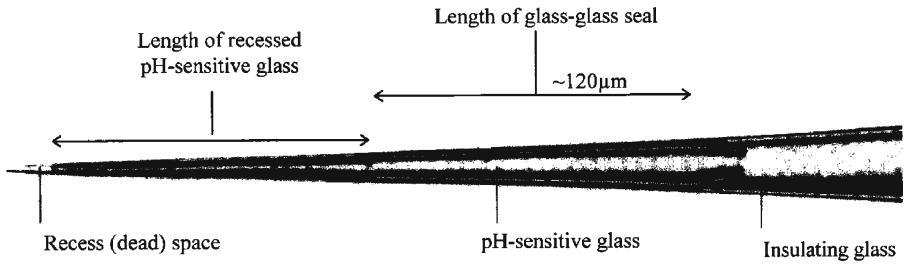

Fig. 2. Recessed-tip pH-sensitive microelectrode as used by Thomas *(20)* to measure intracellular pH in snail neurons. Reproduced from ref. *(20)* with permission from PMC.

μm in length) was recessed within the insulating glass such that the pH of the recessed space was measured. The tip diameters of the completed pH-sensitive microelectrodes were <1 μm. The result was that only the 1- to 2-μm tip had to be placed within the cell. Such microelectrodes require considerable skill to manufacture. The recessed-tip pH-sensitive microelectrode has been used to measure intracellular pH in numerous cell types (snail neurons, skeletal muscle, and cardiac muscle), and despite its relatively slow response, for those who can produce them, it remains the method of choice for measuring intracellular pH in cells approximately 100 μm in diameter. Even with such large cells, the requirement to place two microelectrodes into one cell can be difficult to fulfill, especially where cell boundaries are obscured. The problems of slow response, large tips, and difficult construction of recessed-tip pH-sensitive microelectrodes have been partially resolved by the discovery of submicron capillary tubes.

At intracellular pH, the ZnO nanorods are positively charged, which provides a suitable environment for the adsorption of low isoelectric point biological function groups (proteins and enzymes) and the retention of bioactivity. In this chapter, we focus on the fabrication of nanostructure ZnO nanorods for intracellular pH sensing. Our main effort has been directed toward the construction of tips capable of penetrating the cell membrane as well as optimization of the electrochemical potential properties. To demonstrate the electrode performance, we use it in biological media. Our results indicate that the electrode acts as an extremely sensitive intracellular pH sensor.

2. Materials

1. Standard buffers: potassium phthalate, pH 4.0; sodium potassium phosphate, pH 6.0; sodium phosphate/potassium phosphate, pH 7.0; hydrochloric acid-borate, pH 8.0; boric

acid-sodium-potassium borate, pH 9.0; and boric acid-sodium-potassium borate, pH 11. Store at room temperature.

2. Buffer solutions having pH values equal to 5.7, 6.1, 6.5, 6.9, 7.3, and 7.7 prepared from sodium phosphate monobasic dehydrate $NaH_2PO_4 \cdot 2H_2O$ and disodium hydrogen phosphate Na_2HPO_4. Store at room temperature.
3. Borosilicate glass capillaries: sterile Femtotip® II with a tip inner diameter of 0.5 μm, an outer diameter of 0.7 μm, and a length of 49 mm (Eppendorf AG, Hamburg, Germany).
4. 0.2 M HCl solution.
5. High-purity silver conductive paint (a division of HK Wentworth Ltd., Kingsburg Park, Midland Road Swadlincote, Derbyshire, DE 11 OAN, UK).
6. Zinc nitrate hexahydrate, reagent grade $[Zn(NO_3)_2 \cdot 6H_2O]$ and hexamethylenetetramine $[(CN_2)_6N_4]$.
7. Ag/AgCl reference electrode from Metrohm (no. 6.0733.100, Zofingen, Switzerland).
8. pH combined electrode from Metrohm (no. 6.0228.020).
9. Pt wire, 10-cm length, for use as anode electrode.
10. DC power supply for applying 1 V potential difference.
11. All electrochemical experiments were carried out using a Metrohm pH meter model 827 at room temperature(22 ± 2°C).
12. Single human adipocyte or fat cells.
13. Nikon inverted microscope for verification that individual cells are probed.
14. Glass slides with dimensions 5 cm × 4 cm × 0.177 mm.

3. Methods

The pH electrode behavior is a function of its extensive interior surface area, whereas that of ZnO nanorods is based on their exterior surface. Assembling many ZnO nanorods together yields the same benefits as the pH electrode (low volume and high reactivity). We use the tip of the electrode surface, which is an important component of electrochemical sensors, for detection. The tip contains hundreds of individual ZnO nanorod sensors. These sensors can be combined to produce a greater level of accuracy for a single proton or hydroxyl group. The pH response of ZnO polar and nonpolar surfaces has been explained in terms of the formation of hydroxyl groups that lead to a pH-dependent net surface charge with a resulting change in voltage at the electrode/liquid interface *(21–24)*. The principle of the ZnO nanorod

electrochemical potential pH sensor shows that when a solid is submerged in a polar solvent or an electrolyte solution, a surface charge will develop. ZnO is an amphoteric oxide in which an electropositive metal atom gives the oxygen a sufficient negative charge to strip a proton from a neighboring H_3O^+. However, the metal ion must be electronegative enough to serve as an electron acceptor from a neighboring OH^-. Theoretically, the potential determining reaction of ZnO nanorods in aqueous solution can be represented by *(25)*:

$$ZnO + 2H^+ + 2e^- = Zn + H_2O. \quad (1)$$

The relation between the ZnO electrode potential difference E and the solution pH is then determined by the Nernst equation:

$$E = E^{o} - \frac{RT}{nF}\ln\left(\frac{f_{\text{Production}}[\text{Production}]}{f_{\text{Reaction}}[\text{Reaction}]}\right) + \frac{2.303RT}{nF}\log(a_{H^+}) - E_{\text{ref}}, \quad (2)$$

where E° is the standard electrode potential of the ZnO redox probe, F is the Faraday constant (96,500 C/mol), T is absolute temperature (298 K), R is the gas constant (8.314 J/mol/K), n is the number of electrons in the redox reaction, a_H is the concentration of protons, E_{ref} is the reference electrode potential, [production] and [Reaction] are the concentrations of species, and $f_{\text{production}}$ and f_{Reaction} are the related activity coefficients. Thus, the plot of the measured open-circuit potential E versus pH shows a Nernstian curve with a theoretical limit of 59.15 mV/pH at 25°C.

3.1. ZnO Nanorods Electrode

A major challenge in producing electrodes for intracellular sensing is tip geometry. Intracellular electrodes must have extremely sharp tips (submicrometer dimensions) and they must be long (>10 μm in length). These characteristics are necessary for effective bending and penetration of the flexible cell membrane.

The intracellular pH measuring method uses two electrodes with ZnO nanorods serving as the intracellular working electrode and Ag/AgCl as the intracellular reference microelectrode (*see* **Fig. 3**). The electrochemical potential difference response recorded in this manner measures the electrochemical surface potential generated near electrodes that may cause voltage differences between the two electrodes. The specific design and fabrication details of the electrochemical potential electrodes are described in **ref.** *(26)*.

Ag/AgCl reference microelectrodes are commonly used to ensure high stability in intracellular probing devices. However, it was suggested that even the reliable Ag/AgCl electrode may fail to support a very high fidelity recording. This may be due

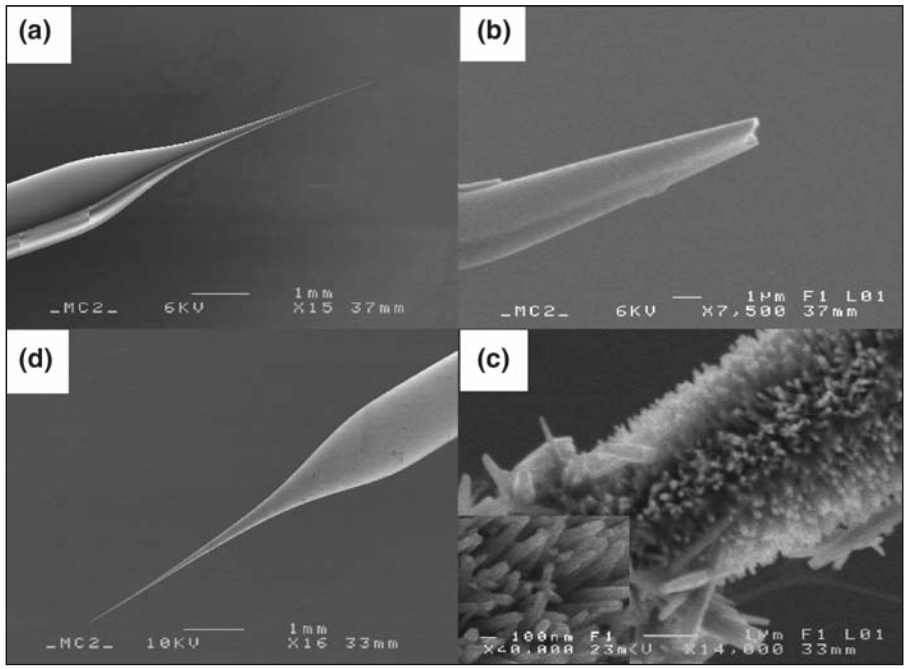

Fig. 3. Ag/AgCl reference microelectrode (**a**) and (**b**) sterile Femtotip II (Eppendorf AG) tip coated with 100-nm silver at different magnifications. (**c**) and (**d**) typical SEM image of the ZnO nanorods grown on Ag coated capillary using low temperature growth at different magnifications. Reproduced from ref.*(26)* with permission from the American Institute of Physics.

to interactions between the silver and organic molecules or an effect related to the miniaturization of the Ag/AgCl electrodes (*see* **Notes 1** and **2**). The Ag/AgCl reference microelectrode was calibrated externally versus an Ag/AgCl bulk reference electrode, which shows approximately constant potential difference using buffer solutions through the pH range 4–11. The fabrication of electrochemical potential ZnO nanorods was performed by the growing of a hexagonal single crystal of ZnO nanorods on silver-coated capillary glass using a low-temperature growth method described previously *(27–29)* (*see* **Notes 1** and **3**). The nanostructure is a rodlike shape with a hexagonal cross section and primarily aligned along the perpendicular direction of the capillary, a typical morphology of wurtzite ZnO structure. The nanorods are uniform in size, with a diameter of 60–80 nm and a length of 500–700 nm.

3.2. Results

3.2.1. Construction of the Electrodes (Potentiometric Measurement)

A two-electrode configuration was used for microliter volumes in electrochemical studies consisting of ZnO nanorods as the working electrode and Ag/AgCl as a reference microelectrode. All electrochemical experiments were conducted using a Metrohm pH meter, model 827 at room temperature (22 ± 2°C).

The response of the ZnO nanorod electrochemical potential difference (as a working electrode versus the Ag/AgCl reference microelectrode) to the changes in standard buffers at room temperature (potassium phthalate pH 4.0, sodium-potassium phosphate pH 6.0, sodium phosphate-potassium phosphate pH 7.0, hydrochloric acid-borate pH 8.0, boric acid-sodium-potassium borate pH 9.0, and boric acid-sodium-potassium borate pH 11) was measured and shows that this pH dependence is linear and has a sensitivity equal to 51.881 mV/pH at 22°C (*see* **Fig. 4**). Electrodes reading less than 50 mV per pH were discarded. The measurements were started immediately after placing the ZnO nanorods and the Ag/AgCl reference microelectrode in the electrolyte drop. To make certain that variations in the tip potential of the reference side caused by differences in the ionic strength of the standard buffers and the cytoplasm of the cell would not cause errors in pH measurement, we tested the electrodes in a potassium phosphate buffer simulating the internal environment of the cell. The measurement duration did not exceed 5 min to avoid significant changes in electrolyte concentration due to evaporation and to maintain the dissolving behavior and stability of the ZnO nanorods *(30)*.

Both the ZnO nanorod pH sensor and the Ag/AgCl reference microelectrode were immersed inside a 30 μL drop of distilled water as a test sample. During data acquisition, a 1-μL drop of 0.1 M HCl or NaOH was added to the distilled water on the glass slide. The signal change from one level to another was recorded, giving the response of the ZnO nanorod pH sensor without stirring (controlled by diffusion to the sensor). We noted that this response was determined both by diffusion to the sensor and within the sensor. The reversibility of the ZnO nanorod pH

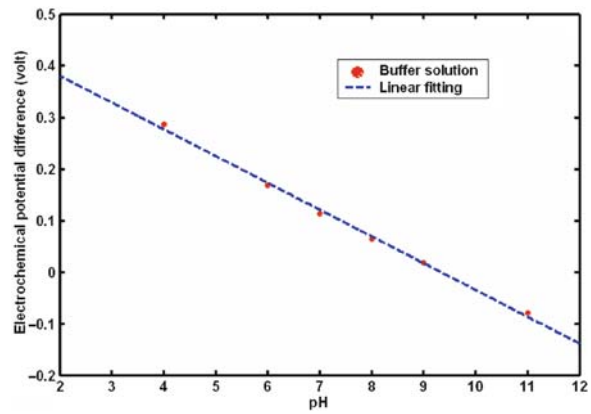

Fig. 4. Calibration curve showing the electrochemical potential difference for the ZnO nanorods as a working electrode with an Ag/AgCl reference microelectrode, versus pH changes for buffer solution. Reproduced from ref.*(26)* with permission from the American Institute of Physics.

sensor is good. The history, i.e., the order of how data are collected, does not affect the electrochemical potential for a specific pH buffer solution. This greatly enhances its ability to work with biological cells, where an abrupt change often occurs and its suitability for applications as a pH mapping sensor.

3.2.2. Intracellular pH in a Single Human Adipocyte or Fat Cell

Cells have multiple mechanisms for intracellular pH regulation that act to adjust pH to changing metabolic conditions. A redundancy of regulatory mechanisms reflects the crucial importance of pH control for cell function and survival, which, to a large extent, depends on enzymes exhibiting more or less distinct pH optima. The control of intracellular pH is thus influenced by such things as hormonal control of cellular function *(31,32)*. There is a particular potential for the local transient control of pH through local production and consumption of protons.

We used the ZnO nanosensor to measure intracellular pH in a single human adipocyte or fat cell *(33)* (*see* **Note 4**). Cells were incubated overnight before use as previously described *(34)*. Informed consent was obtained from all participating individuals and the procedures were approved by the local ethics committee. A glass slide substrate (5 cm in length, 4 cm in width, and 0.17 mm in thickness) with sparsely distributed fat cells was placed on the prewarmed microscope stage set at 37°C. The pH nanoelectrode, mounted on a micropipette holder of a micromanipulation system, was moved into position in the same plane as the cells. The ZnO nanoelectrode and reference electrodes were then gently micromanipulated into the cell using the hydraulic fine adjustments. They were inserted past the cell membrane and extended a short way into the cell. A signal reading was taken with the nanoelectrode inside the cell (pH = 6.81) (*see* **Fig. 5**). Once the ZnO nanorod working electrode and the Ag/AgCl reference microelectrode were inside the cell, the electrochemical potential difference signal detected and identified the proton activity (pH). The pH signal generated was detected with a Metrohm pH meter, model 827. Additionally, the entire experiment was imaged using a charge-coupled device (CCD) camera coupled to the side port of the Nikon inverted microscope, as verification that individual cells were probed. A typical experimental measurement required approximately 5 min. In this work, we found the measured pH value (6.81) to be close to reported values for intracellular pH, 6.95–7.57 in rat brown adipocytes *(31)* or 6.85–7.05 in rat hepatocytes *(35)* using an indirect determination of pH.

3.2.3. Cell Viability

Undoubtedly, placing pH microelectrodes inside cells causes some damage, but the membrane potential is measured and the damage can be assessed. The damage usually consists of a "leak" around the electrodes. This leak rarely causes a large change in intracellular pH because the intracellular buffering power is high

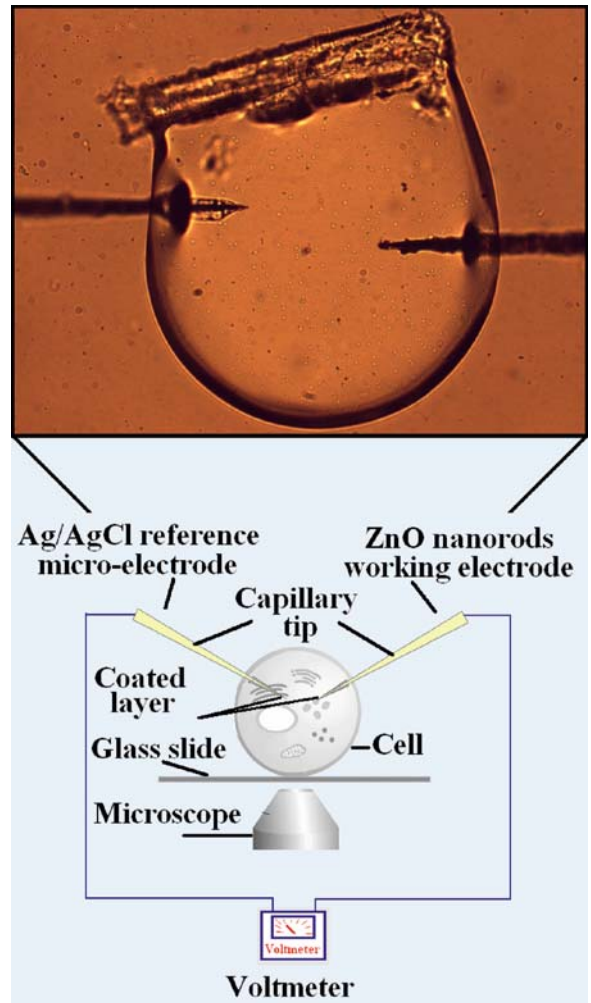

Fig. 5. Optical image and schematic diagram illustrating intracellular pH measurements performed in a single human fat cell using ZnO nanorods as a working electrode with an Ag/AgCl reference microelectrode. Reproduced from ref. *(26)* with permission from the American Institute of Physics.

and the pH gradient across the cell membrane is low. The extent to which the membrane potential reflects the amount of damage is, of course, dependent on the input resistance of the cell. The damage to large cells is less than the damage to small cells. However, in both small and large cells, the damage, if sufficient, will lead to a large influx of other ions, such as calcium and sodium. This physical damage to the integrity of the cell membrane has limited the used of pH microelectrodes to large cells and represents a constant source of anxiety for those using ion-sensitive microelectrodes.

The viability of the penetrated cells depends strongly on the size of the ZnO nanorods. We used ZnO nanorods (80 nm in

diameter and 700 nm in length) grown on one side of the capillary glass with a 0.7-μm tip diameter, so the total diameter of the tip is 1.5 μm. By reducing the size of the ZnO nanorods, the total diameter of the tip was reduced, which, in turn, increased cell viability and the sensitivity of the device increases. Increasing the size of the ZnO nanorods to 500–600 nm in diameter and 3–5 μm in length caused the cells to die immediately (*see* **Fig. 6**).

The introduction of ZnO nanorod pH sensors into a single cell's cytoplasm to measure the intracellular pH does not visibly seem to affect cellular viability. This has been empirically established in several experiments in which, after ZnO nanorod penetration and equilibration for 5 min, the electrode was withdrawn and the cells were monitored by microscope. This study demonstrated that ZnO nanorods are minimally invasive tools appropriate for monitoring pH changes inside living cells.

3.2.4. Probe Usability

The ZnO nanorod electrode was used to obtain only one measurement at a time and was not reused. We made calibration measurements of the solution surrounding the cell after the measurement inside the cell to obtain a quantitative estimation of the detection signal. For these calibration measurements, the ZnO nanorod electrode was placed in the solution surrounding cells directly after the intracellular measurement, and a pH reading of 6.77 was obtained where the actual pH value of the surrounding solution was 7.4. We think that the difference between actual and measured pH values resulted from the strong association of cell materials with the electrode (*see* **Fig. 7**).

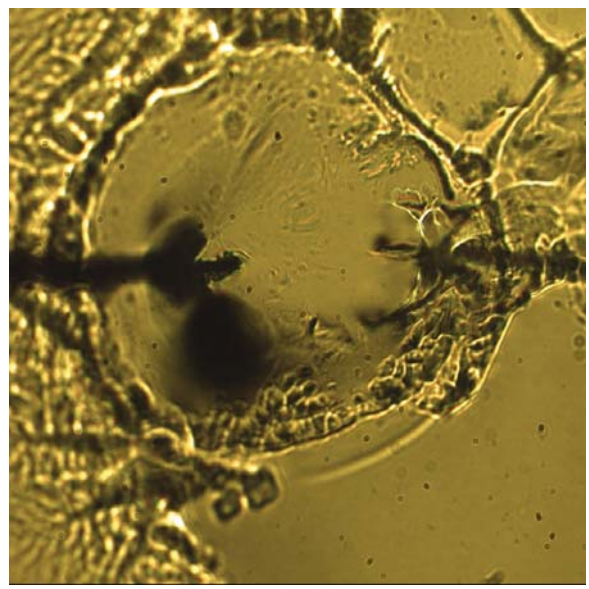

Fig. 6. Dead adipocyte during the intracellular pH measurement using a ZnO electrode.

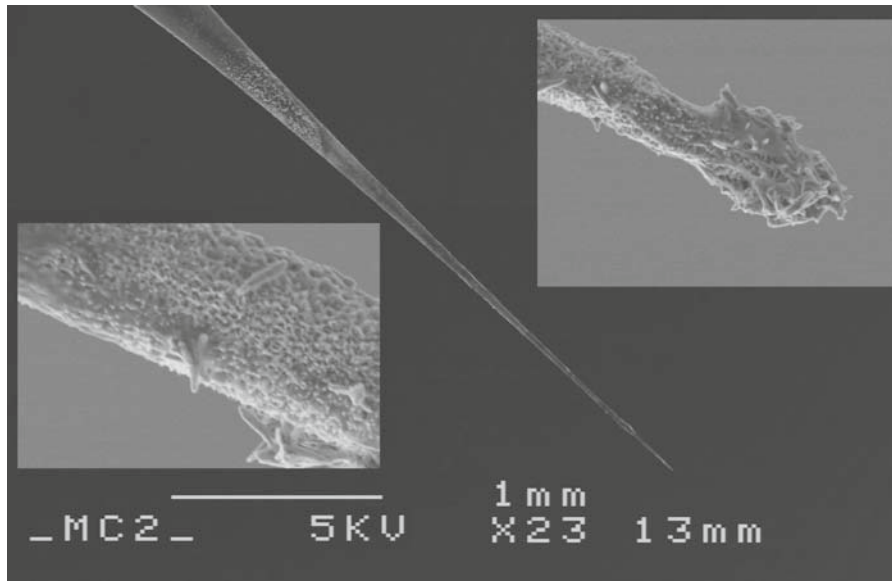

Fig. 7. The strong association of binding to cell materials with the ZnO nanorod electrode after the experiment. Reproduced from ref. *(26)* with permission from the American Institute of Physics.

4. Notes

1. Sterile borosilicate glass capillaries (Femtotip® II) were fixed on a flat support in the vacuum chamber of a sputtering system (AVAC HVC 600 e-beam evaporator), so that a thin silver film with a thickness of 100 nm was uniformly deposited onto their outer surface.
2. By introducing some optimization steps, the AgCl tip coating was prepared electrochemically by dipping the coated end of a capillary in 0.2 M HCl solution and then the silver film was electrolyzed to form AgCl by polarizing it at 1.0 V for 30 s. A 3-cm-long Ag/AgCl layer was coated on the tip of the capillary to serve as a reference electrode, leaving 3 mm of Ag/AgCl exposed at the very tip. The remainder of the Ag/AgCl layer was coated with insulation. The other end of the Ag/AgCl layer was connected with a copper wire (0.5 mm in diameter and 10 cm in length) and fixed by means of high-purity silver conductive paint.
3. The construction of ZnO nanorods working electrode was made by the growing of ZnO nanorods on silver-coated capillary glass using a low-temperature growth method described previously in the text. ZnO nanorods were grown on borosilicate glass Femtotip® II capillary coated with silver film. The ZnO

nanorods cover 3 mm of the silver-coated film that is 3-cm long. The electrical contacts are made by deposition of gold-coated film (100 nm thickness and 1 cm length) on the other end of the Ag film and then connected to the 0.5-mm-diameter insulated copper wire using high-purity silver conductive paint.

4. The cells were isolated by collagenase digestions of pieces of subcutaneous adipose tissue obtained during elective surgery at the University Hospital in Linköping.

Acknowledgments

The authors gratefully acknowledge the financial support from the Swedish Research Council and Molecular Skin Research Platform within the Faculty of Science at Göteborg University.

References

1. Zheng, G., Patolsky, F., Cui, Y., Wang, W. U., and Lieber, C. M. (2005). Multiplexed electrical detection of cancer markers with nanowire sensor arrays. *Nature Biotechnology* **23**, 1294–1301
2. Cui, Y., Wei, Q., Park, H., Lieber, C. M. (2001). Nanowire nanosensors for highly sensitive and selective detection of biological and chemical species. *Science* **293**, 1289–1292
3. Popovtzer, R., Neufeld, T., Ron, E. Z., Rishpon, J., and Shacham-Diamand, Y. (2006). Electrochemical detection of biological reactions using a novel nano-bio-chip array. *Sensors and Actuators B* **119**, 664–672
4. Cai, X., Klauke, N., Glidle, A., Cobbold, P., Smith G. L., and Cooper, J. M. (2002). Ultra-low-volume, real-time measurements of lactate from the single heart cell using microsystems technology. *Analytical Chemistry* **74**, 908–914
5. Zwicker, G. and Jacobi, K. (1983). Site-specific interaction of H2O with ZnO single-crystal surfaces studied by thermal desorption and UV photoelectron spectroscopy. *Surface Science* **131**, 179–194
6. Parker, T. M., Condon, N. G., Lindsay, R., Leibsle, F.M., and Thornton, G. (1998). Imaging the polar $(000\bar{1})$ and non-polar $(10\bar{1}0)$ surfaces of ZnO with STM. *Surface Science* **415**, L1046–L1050
7. Matsunaga, K., Oba, F., Tanaka, I., and Adachi, H. (1999). Valence band structure of ZnO (1010) surface by cluster calculation. *Journal of Electroceramics* **4**, 69–80
8. Wander, A. and Harrison, N. M. (2001). The stability of polar oxide surfaces: The interaction of H_2O with ZnO (0001) and ZnO$(000\bar{1})$. *Journal of Chemical Physics* **115**, 2312–2316
9. Wander, A., Schedin, F., Steadman, P., Norris, A., McGrath, R., Turner, T.S., Thornton, G., and Harrison, N. M. (2001). Stability of polar oxide surfaces. *Physical Review Letters* **86**, 3811–3814
10. Dulub, O., Boatner, L. A., and Diebold, U. (2002). STM study of the geometric and electronic structure of ZnO (0001)-Zn, $(000\bar{1})$-o,$(10\bar{1}0)$, and $(11\bar{2}0)$ surfaces. *Surface Science* **519**, 201–207
11. Kresse, G., Dulub, O., and Diebold, U. (2003). Competing stabilization mechanism for the polar ZnO(0001)-Zn surface. *Physical Review B* **68**, 245409–(15 pages)
12. Dulub, O., Diebold, U., and Kresse, G. (2003). Novel stabilization mechanism on polar surfaces: Zn(0001)-Zn. *Physical Review Letters* **90**, 016102–(4 pages)

13. Meyer, B., Marx, D., and Dulub, O. (2004). Partial dissociation of water leads to stable superstructures on the surface of zinc oxide. *Angewandte Chemie (International ed. in English)* **43**, 6642–6645
14. Meyer, B. (2004). First principles study of the polar O-terminated ZnO surface in thermodynamic equilibrium with oxygen and hydrogen. *Physical Review B* **69**, 045416–(10 pages)
15. Dulub, O., Meyer, B., and Diebold, U. (2005). Observation of the dynamical in a water monolayer adsorbed on a ZnO surface. *Physical Review Letters* **95**, 136101–(4 pages)
16. Glab, S., Hulanicki, A., Edwall, G., and Ingman, F. (1989) Metal-metal oxide and metal oxide electrodes as pH sensors. *Analytical Chemistry* **21**, 29–46
17. Cammann, K., Ross, B., Katerkamp, A., Reinbold, J., Grundig, R., and Renneberg, R. (2002). Chemical and Biochemical Sensors. Wiley-VCH verlag GmbH & Co. KGaA, Ullmann's encyclopedia of industrial chemistry
18. Wang, H., Nakamura, H., Yao, K., Uehara, M., Nishimura, S., Maeda, H., and Abe, E. (2002). Effect of polyelectrolyte dispersants on the preparation of silica-coated zinc oxide particles in aqueous media. *Journal of the American Ceramic Society* **85**, 1937–1940
19. Caldwell, P. C. (1954). An investigation of the intracellular pH of crab muscle fibres by means of micro-glass and micro-tungsten electrode. *Journal of Physiology* **126**, 169–180
20. Thomas, R. C. (1974). Intracellular pH of snail neurons measured with a new pH-sensitive glass micro-electrode. *Journal of Physiology* **238**, 159–180
21. Yan, Y. and Al-Jassim, M. M. (2005). Structure and energetics of water adsorbed on the ZnO($10\bar{1}0$) surface. *Physical Review B* **72**, 235406–(6 pages)
22. Martins, J. B. L., Longo, E., Salmon, O. D. R., Espinoza, V. A. A., and Taft, C. A. (2004).w The interaction of H2, CO, CO2, H2O and NH3 on ZnO surfaces: an Oniom study. *Chemical Physics Letters* **400**, 481–486
23. Martins, J. B. L., Andres, J., Longo, E., and Taft, C. A. (1996). Properties, dynamics, and electronic structure of condensed systems H2O and H2 interaction with ZnO surfaces: A MNDO, AM1, and PM3 theoretical study with large cluster models. *International Journal of Quantum Chemistry* **57**, 861–870
24. Martins, J. B. L., Moliner, V., Andres, J., Longo, E., and Taft, C. A. (1995). A theoretical study of water adsorption on ($10\bar{1}0$) and (0001) ZnO surfaces: molecular cluster, basis set and effective core potential dependence. *Journal of Molecular Structure (Theochem)* **330**, 347–351
25. Stumm, W. and Morgan, J. J. (1981). Precipitation and dissolution. In: Aquatic Chemistry: An Introduction Emphasizing Chemical Equilibria in Natural Waters. (John Wiley&Sons), New York, pp. 230–322
26. Al-Hilli, S., Öst, A., and Strålfors, P., and Willander, M. (2007). ZnO nanorods as an intracellular sensor for pH measurements. *Journal of Applied Physics* **102**, 084304–(5 pages)
27. Greene, L. E., Law, M., Goldberger, J., Kim, F., Johnson, J. C., Zhang, Y., Saykally, R. J., and Yang, P. (2003). Low-temperature wafer-scale production of ZnO nanowire arrays. *Angewandte Chemie (International ed. in English)* **42**, 3031–3034
28. Vayssieres, L., Keis, K., Lindquist, S., and Hagfeldt, A. (2001). Purpose-built anisotropic metal oxide material: 3D highly oriented microrod array of ZnO. *The Journal of Physical Chemistry B* **105**, 3350–3352
29. Li, Q., Kumar, V., Li, Y., Zhang, H., Marks, T. J., and Chang, R. P. H. (2005). Fabrication of ZnO nanorods and nanotubes in aqueous solutions. *Chemistry of Materials* **17**, 1001–1006
30. Zhou, J., Xu, N., and Wang, Z. L. (2006). Dissolving behavior and stability of ZnO wires in biofluids: a study on biodegradability and biocompatibility of ZnO nanostructures. *Advanced Materials* **18**, 2432–2435
31. Lee, S. C., Hamilton, J. S., Trammell, T., Horwitz, B., and Pappone, P. A. (1994). Adrenergic modulation of intracellular pH in isolated brown fat cells from hamster and rat. *American Journal of Physiology Cell Physiology* **267**, C349–C356
32. Shrode, L. D., Tapper, H., and Grinstein, S. (1997). Role of intracellular pH in proliferation, transformation, and apoptosis. *Journal of Bioenergetics and Biomembranes* **29**, 393–399
33. Strålfors, P. and Honno, R. C. (1989). Insulin-induced dephosphorylation of hormone-sensitive lipase-correlation with lipolysis and cAMP-dependent protein kinase activity. *European Journal of Biochemistry* **182**, 379–385
34. Danielsson, A., Öst, A., Lystedt, E., Kjolhede, P., Gustavsson, J., Nystrom, F. H., and Strålfors, P. (2005). Insulin resistance in human adipocytes occurs downstream of IRS1 after surgical cell isolation but at the level of phosphorylation of IRS1 in type 2 diabetes. *FEBS Journal* **272**, 141–151
35. Pollock, A.S. (1984). Intracellular pH of hepatocytes in primary monolayer culture. *American Journal of Physiology. Renal Physiology* **246**, F738–F744